

ZnS (Mn) Nanoparticles as Luminescent Centers for Siloxane Based Scintillators

S. CARTURAN^{1,2}, G. MAGGIONI^{1,2}, M. CINAUSERO², T. MARCHI^{2,3},
F. GRAMEGNA², F. PINO^{1,4}, D. FABRIS², A. QUARANTA^{5,6}, L. SAJO-BOHUS^{1,4}

¹Dipartimento di Fisica dell'Università di Padova, Padova, Italy.

²INFN, Laboratori Nazionali di Legnaro, Legnaro (Padova), Italy.

³Institute for Nuclear and Radiation Physics, Leuven, The Netherlands.

⁴Department of Physics, University Simon Bolivar, Baruta, Venezuela.

⁵Department of Industrial Engineering, University of Trento, Trento, Italy.

⁶INFN-TIFPA, Sezione di Trento, Trento.

Email: sara.carturan@lnl.infn.it

Published online: August 08, 2016,

The Author(s) 2016. This article is published with open access at www.chitkara.edu.in/publications

Abstract Synthesis of oleic acid stabilized ZnS nanocrystals activated with Mn is pursued. A hydrothermal method where high pressure and temperature are applied to control the nanocrystals growth is adopted. Capping the nanoparticle surface with oleic acid (OA) improved light output. Samples loaded with both the phosphor and the neutron sensitizer have been produced and tested in a preliminary test as alpha particle detectors and secondly as thermal neutron detectors. The results support further development for siloxane-based scintillator detectors employing ZnS (Mn) nanoparticles.

Keywords: neutron detector, scintillator, nanoparticle, ZnS(Mn)

1. INTRODUCTION

The detection of thermal neutrons by simple and reliable methods is currently highly requested in several fields. Besides the highly efficient, reliable and γ -rays insensitive ³He based system, the most widely used thermal neutron detectors are based on ⁶Li glass (Appl. Scint. Techn., UK) and Ag activated ZnS screens added with ⁶LiF for neutron absorption and conversion (Eljen Technology, Scionix, Holland). Recently, siloxane scintillators doped with o-carborane displayed good response to thermal neutron, owing to the high cross section of ¹⁰B to thermal neutrons (38380 barns) and high solubility of

Journal of Nuclear
Physics, Material
Sciences, Radiation and
Applications
Vol-4, No-1,
August 2016
pp. 107–116

Carturan, S.
Maggioni, G.
Cinausero, M.
Marchi, T.
Gramegna, F.
Pino, F.
Fabris, D.
Quaranta, A.
Sajo-Bohus, L.

o-carborane within the silicone base resin (up to 8% wt.) with maintenance of both mechanical and optical features [10,2].

The use of ${}^6\text{Li}$ as neutron converter could potentially offer great benefit over ${}^{10}\text{B}$ in spite of the lower capture cross section since two ionizing particles (triton and proton) are produced back to back with higher total energy (about 4.8 MeV). Moreover, no undesirable γ -rays cascade is produced as a by-product of the nuclear reaction. Screens based on ZnS are known since the far 1900. Their typical features are intense light yield (up to 100.000 photons/MeV [8]), ease of signal detection (λ_{em} is around 450 nm, in the blue region, where common photomultiplier tubes can be used) and low cost. The neutron converter ${}^6\text{LiF}$ is mixed in form of micron-sized powders with ZnS (Ag) powder and a binder (epoxy resin) to provide a reliable neutron detection system. However, carefully controlled manufacturing is required to assure complete reproducibility as for grains size homogeneity and uniformity of the two phases. In fact, it has been recently proved that the phosphor grains size has great influence on the final light yield, owing to the small path, in the order of microns, of the alpha particle produced from neutron capture on ${}^6\text{Li}$ [6]. The use of nanoparticles for both the phosphor and the neutron absorber compounds could greatly improve the mixture homogeneity and could provide enhanced light output.

In this work, the synthesis of oleic acid stabilized ZnS nanocrystals activated with Mn is pursued. Fluorescence emission is known to be strongly enhanced in the case of surface capping of nanoparticles, as a result of defects passivation in the structure of the nanocrystals [12,5]. A hydrothermal method where high pressure and temperature are applied to control the nanocrystals growth is adopted. Capping the nanoparticle surface with oleic acid (OA) can hamper agglomeration and, meanwhile, can be useful to improve the compatibility with the binder. As a first attempt, the nanoparticles will be dispersed in polysiloxane, which is known to afford good mechanical strength, optical transparency and radiation resistance [1,3]. The successful synthesis of ${}^6\text{LiF}$ nanoparticles capped with OA has been already reported and entrapment of those nanoparticles into polysiloxane based scintillators, doped with organic dyes, proved to be sensitive to thermal neutrons, giving rise to a clear signal, though increase in light output should be desirable [11].

In the present work, samples loaded with the OA stabilized nanocrystals of both ZnS activated with Mn and neutron sensitizer ${}^6\text{LiF}$ have been produced and tested. In a first experiment, only ZnS based nanoparticles have been included in polysiloxane, in order to characterize their capability to detect alpha particles, which are indeed one of the products of the reaction capture

of thermal neutrons on ${}^6\text{Li}$ nucleus. Then, a first attempt of loading the base siloxane with both the phosphor and the neutron converter has been pursued, in order to monitor the response of the scintillator towards thermal neutrons.

2. EXPERIMENTAL

The synthesis of nanoparticles has been performed following a previously reported method [4,13]. In a typical synthesis, zinc acetate and manganese acetate were added into deionized water. Then, sodium sulfide was dissolved into deionized water to form a transparent solution. The first solution was transferred to an autoclave and oleic acid, sodium oleate and ethanol were added. Then, the sulfide solution was added and the autoclave was sealed and maintained at 190 °C for 12 h. The resulting ZnS (Mn) nanoparticles were washed with ethanol/cyclohexane mixture to remove the excess of oleic acid. Siloxane samples with thickness of about 0.5 mm have been obtained by dissolving either 5% or 10% wt. of ZnS (Mn) into the base resin and carrying out the cross-linking reaction as usual [10,2]. Samples loaded also with ${}^6\text{LiF}$ OA were also prepared for the test with thermal neutrons, following a previously described procedure [11].

3. NEUTRON EFFICIENCY AS ESTIMATED BY GEANT4

Monte Carlo simulations offer an important tool in the design of nuclear detection systems and it is therefore interesting to assess the capability of such calculation. Hence, in this work GEANT4 10.01 toolkit [9,7] was used to determine the response of the detector scintillator with the following stoichiometry ratio: Zn 0.05, S 0.05, Mn 0.0015, Li 0.2, F 0.2, Si 1.0, C 3.6, O 1.0, H 7.2 (for the samples containing 0.5 wt% ${}^6\text{Li}$). Since the density of the material is 1.03 g/cm³, samples with 0.5 wt% contain 5×10^{20} atoms/cm³ of ${}^6\text{Li}$, while in the standard glass GS20 the concentration is 1.6×10^{22} atoms/cm³. In particular, it was estimated the neutron efficiency of the detector for two different thickness. GEANT4 offers access to particle tracking (e.g. position/time of the particle, kinetic energy, deposited energy, etc.) through the “G4Track.hh” class. It was used to determine the amount of neutron capture reactions on ${}^6\text{Li}$ and to check if the reaction products (${}^3\text{H}$ and alpha) deposit all their energy into the sensitive material.

The simulated geometry consisted into a disk of diameter $F = 2.54$ cm with a thickness equal to 0.5 or 1.0 mm. The chemical (and isotopic) composition of the sensitive material was introduced following its real one. A mono-energetic parallel neutron beam impinging on the detector was simulated, with energies between 10^{-3} eV and 1 MeV. In order to get a good statistic, 10^6 primary particles were simulated. It was used a physics list that includes the high precision neutron

Carturan, S.
Maggioni, G.
Cinausero, M.
Marchi, T.
Gramegna, F.
Pino, F.
Fabris, D.
Quaranta, A.
Sajo-Bohus, L.

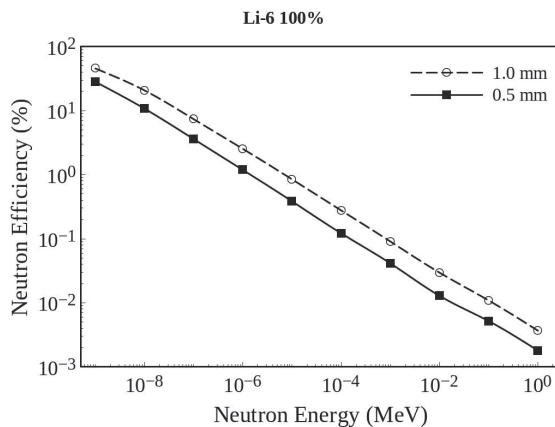


Figure 1: Neutron efficiency for two scintillator detectors with ${}^6\text{Li}$ 0.5 wt %.

package (NeutronHP) to transport neutrons below 20 MeV down to thermal energies. The neutron efficiency curves of the detector, for different thickness and the same ${}^6\text{Li}$ concentration (0.5 wt %), are shown in Fig. 1. From these results it can be deduced that the efficiency in thermal neutrons capture approaches 100% for the case of both thickness and for the present scintillator composition.

However, it is important to observe that this efficiency is far from being related to the efficiency of detection, which is indeed correlated to the light output of the scintillating disk when irradiated with a real moderated neutron source. Light generation from alpha and tritons produced inside a nanocluster of ${}^6\text{LiF}$ molecules and impinging on the neighboring ZnS:Mn luminescent centers is quite difficult to simulate as too many parameters such as opacity, grain size, light scattering, light absorption, light loss at the disk edges should be taken into account. Modeling this type of system is quite complicated and it is beyond the scope of the present work.

4. RESULTS

The HRXRD patterns of the prepared oleic acid stabilized ZnS (Mn) powders with ZnS (Mn) 100:1 and 100:2.7 molar ratios are reported in Fig. 2.

The main peaks of cubic zinc blend structure (111), (220), (311) are observed and indexed in the graph of Fig. 2. It is worth to note that doping the nanoparticles of ZnS with ions Mn does not change the diffraction pattern of the bare ZnS crystal, and no peaks corresponding to Mn precipitates or Mn -related impurity phase were observed, thus confirming the formation of a ZnS (Mn) solid solution without observable phase separation. This result points to

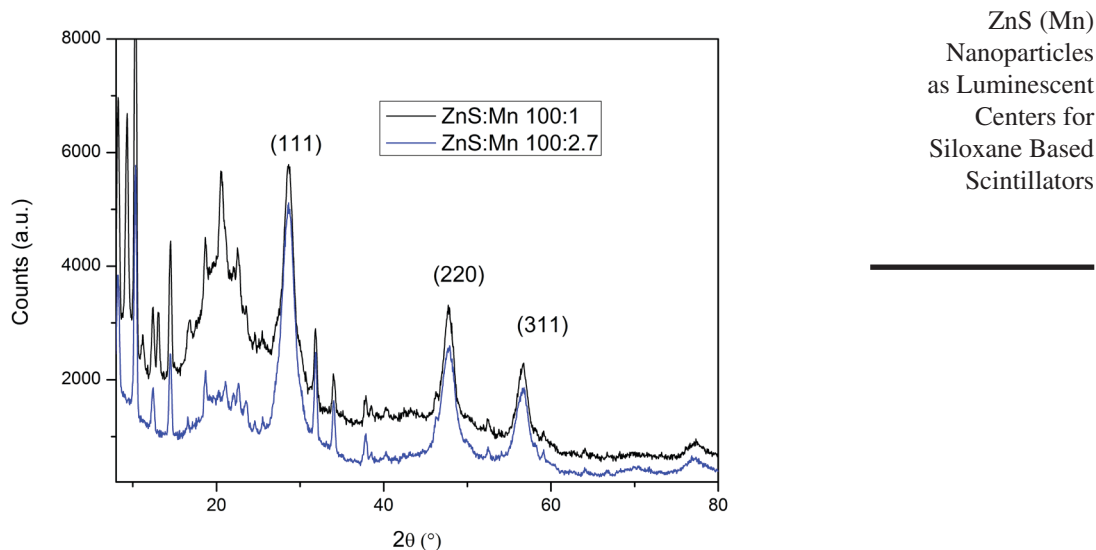


Figure 2: HRXRD patterns from ZnS(Mn) powders.

the entrapment of Mn^{2+} ions inside the nanocluster, as a substitutional atom, and not simply bound on the surface of ZnS nanocrystals. Using the full width at half-maximum of the reflection from the (111) plane, the mean crystallite size of ZnS (Mn) was estimated as 6.3 nm (100:1) and 4.8 nm (100:2.7), applying the Scherer formula.

Photoluminescence (PL) spectra of the siloxane loaded samples with a fixed amount of ZnS (Mn) and different molar ratio between ZnS and Mn are shown in Fig. 3 (λ of excitation was fixed at 340 nm).

The emission of ZnS (Mn) nanoparticles is observed at 430 nm and 590 nm, in agreement with literature data, where the orange emission is attributed to the ${}^4T_1 \rightarrow {}^6A_1$ transition of Mn^{2+} [4,13]. The increase in intensity of the orange emission band versus the blue one increases with the amount of Mn activation level, though amounts higher than 2.7% displays a drop in luminescence at 590 nm, thus proving that too high a doping level causes enhanced non-radiative deactivation pathways. Moreover, it was reported that in case of Mn^{2+} ions incorporated within the nanocrystals, both the 435 nm blue emission of ZnS and the orange Mn^{2+} emission at 590 nm are visible, differently from the case of surface localized Mn ions, where only the blue luminescence is observed [13]. Therefore, it can be concluded from XRD results and photoluminescence spectra that using the present synthesis good results as for structural distribution of the dopant and enabled energy

Carturan, S.
Maggioni, G.
Cinausero, M.
Marchi, T.
Gramegna, F.
Pino, F.
Fabris, D.
Quaranta, A.
Sajo-Bohus, L.

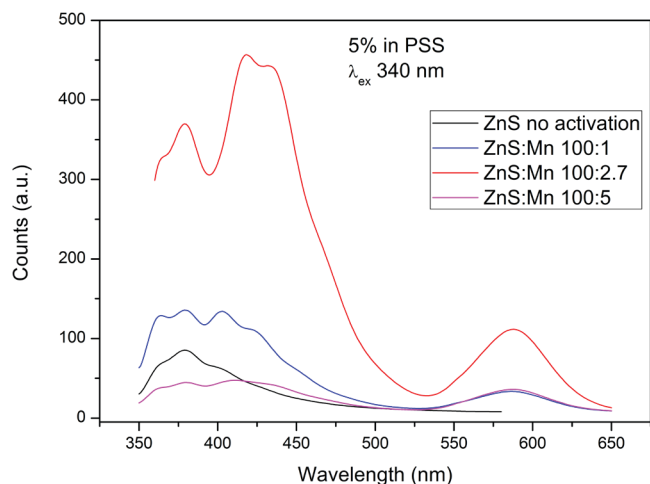


Figure 3: Photo luminescence spectra of ZnS (Mn) containing samples.

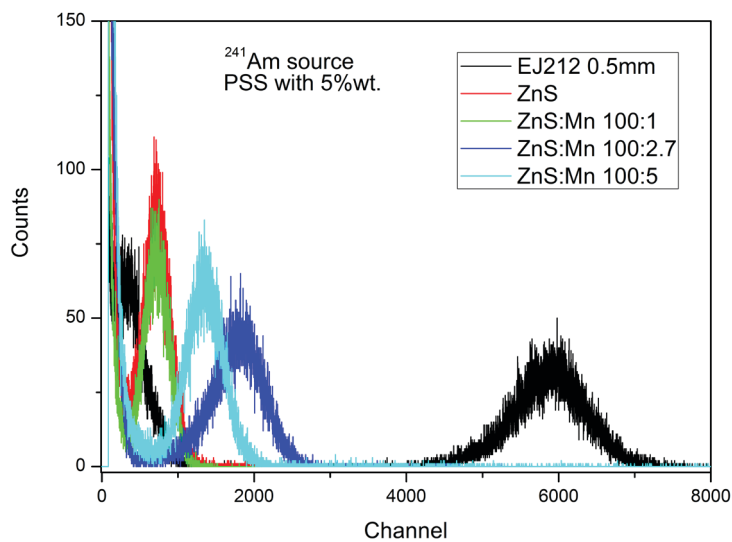
transfer from the excited level of the base ZnS crystal and Mn^{2+} interband level can be achieved.

In order to test the detection ability of these luminescent disks towards alpha particles, the samples have been irradiated with ^{241}Am source and the obtained pulse-height spectra, as compared to the standard plastic scintillator EJ212, are reported in Fig. 4.

The light output is low as compared with EJ212, the maximum value being about 30% of the standard. This observation can be ascribed to the opacity of the samples, as clearly seen in the samples photo of Fig. 5. As a matter of fact, alpha particles can travel only few tens of microns within the siloxane pellet, producing excitation in the luminescent centres in that precise slice of material. Then, light propagation should occur through several hundreds of microns in the case of 0.5 mm thick pellet and a remarkable light loss during this path can be expected. Therefore, though the capping with oleic acid yields a remarkable improvement in dissolution capability, the opacity induced by addition of inorganic nanoparticles is still an issue to be addressed.

Nevertheless, a fair sensitivity toward ionizing particles is demonstrated by these new scintillators as shown by the collected signals reported in Fig. 4, hence a first attempt to obtain a visible signal from thermal neutrons irradiation has been made.

Samples obtained from the cross-linking of the base polysiloxane resin and containing both the inorganic luminescent centers (ZnS:Mn 100:2.7) and 6LiF



ZnS (Mn)
Nanoparticles
as Luminescent
Centers for
Siloxane Based
Scintillators

Figure 4: Pulse-height spectra obtained from ZnS (Mn) loaded in PSS samples irradiated with alpha particles.

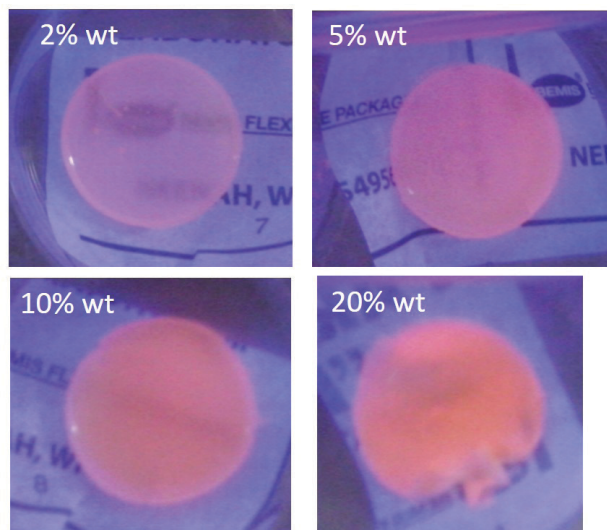


Figure 5: Photos of ZnS (Mn) and ^6LiF doped samples of siloxane under UV light illumination.

Carturan, S.
Maggioni, G.
Cinausero, M.
Marchi, T.
Gramegna, F.
Pino, F.
Fabris, D.
Quaranta, A.
Sajo-Bohus, L.

oleic acid capped nanoparticles have been prepared. The mass ratio between ZnS (Mn) and ${}^6\text{LiF}$ has been fixed at 1:1, while the weight of added powders to siloxane has been varied between 2 and 20%.

Thermal neutrons from a polyethylene blocksmoderated ${}^{252}\text{Cf}$ source have been used to irradiate samples containing both ZnS (Mn) and ${}^6\text{LiF}$. Unfortunately, poor detector response was obtained, irrespective of the used concentration of phosphor or neutron converter concentration. This result is most probably due to the intrinsically low light output of the Mn activated ZnS nanoparticles. As a matter of fact, in this case the ionizing particles, alpha and tritons, are locally generated from n-capture on ${}^6\text{Li}$ nucleus and emitted back to back towards the luminescent centres. However, the pathway of the primary particles can be seriously hampered by the presence of oleic acid molecules or by scattering with other LiF molecules located close to the emitting centre. Hence, excitation through primary or secondary particles of the active centre is not straightforward and very high light yield from the bare luminescent particle in itself is mandatory in order to get sufficient light output from the thin disk. In the case of commercial objects, the well-known high light yield of ZnS is exploited to collect the moderate light emitted at the very bottom of the disk in contact with the photomultiplier tube window. In fact, the opacity of the scintillator causes self-absorption and light loss, so that only a very limited volume can be considered active as emission source. Light emission from the nanoparticles could be improved by using different surface nanoparticles stabilizer, such as methacrylic acid or polymethyl methacrylate instead of oleic acid, and by increasing the homogeneity of the dispersion to avoid particles agglomeration using ultrasonic probes or shear mixers during the samples preparation.

5. CONCLUSIONS

In the present work a novel type of scintillator has been prepared using as base resin a polysiloxane with intrinsic features of transparency, mechanical robustness and radiation resistance. The luminescent centres are inorganic nanoparticles composed of ZnS activated with Mn ions. The synthesis has been conducted following a hydrothermal method in oleic acid environment, in order to control the size and the structure of the nanoparticles, meanwhile stabilizing the surface of the nanocrystals with oleic acid molecules. This approach leads to more soluble active luminescent centres inside the polymer-base matrix, thus increasing the overall transparency. Moreover, the presence of oleic acid on the surface of the nanoparticles can hinder agglomeration, thus giving rise to a more homogeneous distribution of the light emission centres in the matrix with

lower effects of light loss due to scattering and self absorption. Different Mn doping levels have been investigated as for light emission under UV excitation and an optimal doping level has been found to enhance the orange emission from Mn interband levels over ZnS blue emission. The produced scintillators proved to respond to alpha particles irradiation, though with moderate light output with respect to commercial organic scintillators. The addition of ${}^6\text{LiF}$ in form of OA nanoparticles has been pursued in order to prove the material as thermal neutron detector. However, the disks appeared even more opaque and white and no response has been detected upon irradiation. This behaviour can be ascribed to the moderate intrinsic light output of the luminescent centres and possible approaches to enhance light yield from these new nanocomposites have been presented.

6. ACKNOWLEDGMENTS

L. Sajo-Bohusis grateful to LNL-INFN for financial support. This work has been financially supported by 3rd and 5th INFN Commissions and by the Ministry of Education (Prin 2010-2011 -2010TPSCSP_005).

REFERENCES

- [1] A. Quaranta, S. Carturan, M. Cinausero, T. Marchi, F. Gramegna, et al. Characterization of polysiloxane organic scintillators produced with different phenyl containing blends. *Mat. Chem. Phys.* 137, 951, (2013). <http://dx.doi.org/10.1016/j.matchemphys.2012.10.041>
- [2] A. Quaranta, S. Carturan, T. Marchi, M. Buffa, M. Degerlier, et al. Doped polysiloxane scintillators for thermal neutrons detection. *J. Non-Cryst. Solids*, 357, 1921-1925, (2011). <http://dx.doi.org/10.1016/j.jnoncrysol.2010.10.043>
- [3] A. Quaranta, S. Carturan, T. Marchi, M. Cinausero, C. Scian, et al. Doping of polysiloxane rubbers for the production of organic scintillators. *Opt. Mat.* 32, 1317-1320, (2010). <http://dx.doi.org/10.1016/j.optmat.2010.04.021>
- [4] B. Dong, L. Cao, G. Su, W. Liu, H. Qu, et al. Synthesis and characterization of the water-soluble silica-coated ZnS:Mn nanoparticles as fluorescent sensor for Cu²⁺ ions. *J Colloid Interface Sci* 339, 78-82, (2009). <http://dx.doi.org/10.1016/j.jcis.2009.07.039>
- [5] G. Murugadoss. Synthesis of ZnS:Mn²⁺ and ZnS:Mn²⁺/ZnS core-shell nanoparticles using poly(methyl methacrylate). *Appl Nanosci* 3 (2013)485–493. <http://dx.doi.org/10.1007/s13204-012-0157-x>
- [6] H. Iwase, M. Katagiri, M. Shibayama. Optimization of the thickness of a ZnS/6LiF scintillator for a high-resolution detector installed on a focusing small-

Carturan, S.
Maggioni, G.
Cinausero, M.
Marchi, T.
Gramegna, F.
Pino, F.
Fabris, D.
Quaranta, A.
Sajo-Bohus, L.

- angle neutron scattering spectrometer (SANS-U). *J. Appl. Cryst.* 45 (2012) 507–512. <http://dx.doi.org/10.1107/S0021889812008928>
- [7] J. Allison, K. Amako, J. Apostolakis, H. Araujo, P. Arce Dubois, et al. Geant4 developments and applications. *IEEE Trans. on Nucl. Sci.* 53 (1), 270-278, (2006). <http://dx.doi.org/10.1109/TNS.2006.869826>
- [8] P. Dorenbos, Light output and energy resolution of Ce³⁺-doped scintillators. *Nucl. Instrum. Meth. A* 486 (2002) 208–213. [http://dx.doi.org/10.1016/S0168-9002\(02\)00704-0](http://dx.doi.org/10.1016/S0168-9002(02)00704-0)
- [9] S. Agostinelli, J. Allison, K. Amako, J. Apostolakis, H. Araujo, et al. Geant4—a simulation toolkit. *Nucl. Inst. and Meth. A* 506, 250-303, (2003). [http://dx.doi.org/10.1016/S0168-9002\(03\)01368-8](http://dx.doi.org/10.1016/S0168-9002(03)01368-8)
- [10] S. Carturan, A. Quaranta, T. Marchi, F. Gramegna, M. Degerlier, et al. Novel polysiloxane-based scintillators for neutron detection. *RadiatProt Dosimetry* 143, 471-476, (2011). <http://dx.doi.org/10.1093/rpd/ncq403>
- [11] S. Carturan, T. Marchi, G. Maggioni, F. Gramegna, M. Degerlier, M. Cinausero, M. Dalla Palma, A. Quaranta. Thermal neutron detection by entrapping 6LiF nanocrystals in siloxane scintillators. *J. Phys. : Conf. Ser.* 620, 012010, (2015) <http://dx.doi.org/10.1088/1742-6596/620/1/012010>
- [12] S.K. Mehta, S. Kumar, M. Gradzielski. Growth, stability, optical and photoluminescent properties of aqueous colloidal ZnS nanoparticles in relation to surfactant molecular structure. *J. Coll. Interf. Sci.* 360 (2011) 497–507. <http://dx.doi.org/10.1016/j.jcis.2011.04.079>
- [13] W. Chen, G. Li, J.-Olle Malm, Y. Huang, R. Wallenberg, et al. Pressure dependence of Mn²⁺ fluorescence in ZnS : Mn²⁺ nanoparticles. *J. Lumin.* 91, 139, (2000). [http://dx.doi.org/10.1016/S0022-2313\(00\)00222-2](http://dx.doi.org/10.1016/S0022-2313(00)00222-2)